Nanoscale

ROYAL SOCIETY OF CHEMISTRY

MINIREVIEW

View Article Online
View Journal | View Issue

Cite this: *Nanoscale*, 2025, **17**, 20848

Optical properties of polymer-derived carbon dots

Yongqi Yang[a] and Deirdre M. O'Carroll *[a,b]

Luminescent carbon dots (CDs), as an emerging material class, have been actively investigated for applications in bioimaging, photocatalysis, and optoelectronic devices. Polymer materials have exhibited great potential as candidates for the preparation of CDs due to the high carbon percentage in their chemical structure and relative abundance. More importantly, chemical upcycling provides an economic approach to process polymer waste. In this article, we review synthetic routes and optical properties of CDs derived from different polymer sources, including polyethylene, polypropylene, mixed polyolefins, polystyrene, polyurethane, polyethylene terephthalate, polyethylene glycol, polylactide, polyacrylamide and polymers derived from natural resources. Applications based on the luminescent properties of these polymer-derived CDs are also briefly discussed. Though most of the current polymer-derived CDs show inferior photoluminescence quantum yields to those of small-molecule-derived CDs, there are pathways to improve the performance of polymer-derived CDs by adjusting the synthetic conditions and incorporating additives or dopants.

Received 14th March 2025,
Accepted 8th August 2025

DOI: 10.1039/d5nr01092f

rsc.li/nanoscale

1. Introduction

Carbon-based materials are a class of high variety and great importance in the field of materials science, while at the same time, they exhibit low-cost and eco-friendly features. Conventional classifications, such as graphite and carbon black, are widely used in fabricating electrodes and supercapacitor devices.[1–4] Graphene and carbon nanotubes received a huge amount of attention due to their unique electronic and chemical properties. Carbon dots (CDs), as quasi-0D carbon-based materials, have also been actively investigated since they were first reported by Xu *et al.* in 2004.[5] The unique optical properties, including tunable photoluminescence (PL),[6,7] and high quantum yield,[8] as well as distinctive low cost and toxicity,[9,10] make CDs promising in many fields, including optoelectronics,[11,12] energy storage,[13,14] catalysis,[15,16] sensors,[17,18] and bioimaging areas.[19] CDs can be prepared from both bottom-up and top-down approaches from different starting materials. Larger-sized carbon materials, such as graphite power, carbon rods and fibers can be processed to synthesize CDs using energy-intensive steps, including laser ablation,[20,21] arc discharge[22] and electrochemical approaches.[23] Organic molecules and carbon-based polymers are the most common raw materials used for preparing CDs by bottom-up methods.[24–26] Citric acid, glucose and aromatic compounds are frequently studied as small-molecule type precursors.[27–30] Carbon-based polymers, such as polyolefins and polyesters, are also candidates for making CDs given their high carbon content. Plastic and natural polymers such as polysaccharide are the most common precursors used due to the large feed stock and low-price. In particular, development of a mature approach to upcycle plastic waste may relieve rising environmental issues and health concerns caused by plastic pollution. In addition, the unique starting structure (linear or cross-linked) of those polymers increases the possibility of preparing CDs of different composition, morphology and properties.

Luminescent properties are important in the study of CDs, as several applications derive from these features. There are three luminescence mechanisms of CDs as proposed in several review articles.[31,32] The first one is the π conjugated domains existing in the carbon core, which alters the bandgap of the original continuous sp^3 structure and allows for exciton production and recombination under suitable excitation.[33] In this scenario, the bandgap is dependent on the conjugation domain size. A theoretical study by Eda *et al.* revealed that the bandgap decreases as the π domain size increases.[34] Considering this effect, the CD system with more heterogeneous size distribution exhibits a broader emission band and excitation-dependent emission behavior. Quantum confinement effects can also cause a size-dependent emission behavior when the particle size is smaller than the exciton Bohr radius.[35] The second mechanism is dependent on the functional groups on the surface of CDs, which usually contain nitrogen or oxygen atoms. Those surface groups can serve as

[a]*Department of Chemistry and Chemical Biology, Rutgers University, 123 Bevier Road, Piscataway, NJ, 08854, USA. E-mail: ocarroll@rutgers.edu*
[b]*Department of Materials Science and Engineering, Rutgers University, 607 Taylor Road, Piscataway, NJ, 08854, USA*

capture centers for excitons, thus giving rise to surface state-related fluorescence.[36,37] However, there are dual roles of the surface functional groups. On one hand, they enable $\pi^* \rightarrow n$ and $\sigma^* \rightarrow n$ transitions, resulting in molecular type PL behavior that is spectrally invariable with change in particle size or excitation energy. On the other hand, they act as energy traps of excitons, just like the defects in the carbon core structure, leading to structure deformation and causing non-radiative decays. Based on this, synthetic methods are sometimes adjusted to add surface passivation reagents as functionalization precursors to enhance PL.[38] The most common passivation molecules on the surface of CDs are mainly amine molecules, such as thiourea,[39] 4,7,10-trioxa-1,13-tridecanediamine (TTDDA),[40] and 1-hexadecylamine.[41] Furthermore, the third mechanism is connected to fluorophores that can also account for the fluorescence of CDs, which usually leads to high photoluminescence quantum yield (PLQY).[42] These fluorophores may exist as a separate byproduct during the synthesis of CDs, which can aggregate into CDs. Crosslink-enhanced emission (CEE) is another specific theory developed for polymeric CDs. Crosslinking can create rigid domains that restrict vibrational and rotational motion of electron-rich heteroatomic groups (*e.g.*, C=O, C=N), suppressing non-radiative decay and enhancing radiative transitions.[43–45] In tightly crosslinked CDs, the proximity between sub-luminophores can induce electron-cloud overlap, splitting intrinsic energy levels into sub-levels.[46] Furthermore, confined-domain CEE helps narrow the singlet–triplet energy gap, promoting intersystem crossing and room-temperature phosphorescence (RTP).[45,47]

Despite extensive trials on upcycling carbon-based polymers into CDs, few of them have clearly established the relationship between reactants and luminescence properties of the products.[44,48] Here, we review recent research on deriving CDs from polymers and categorize them based on the type of starting materials with a focus on the products' photoluminescent properties. Applications based on the luminescent properties of polymer-derived CDs are also discussed and their performance is compared with counterparts derived from small organic molecules.

2. Optical properties of polymer-derived CDs and their relationship to the starting material

2.1. Polyethylene (PE)

Plastic bags are the most common polyethylene source to prepare PE-derived CDs as reported. Abdelhameed *et al.* synthesized CDs from PE bags with a one-step oxidative hydrothermal reaction, where diluted nitric acid was employed as the oxidant and solvent.[49] A two-step reaction mechanism was proposed: (1) PE or polypropylene (PP) polymers undergo degradative oxidation to a mixture of dicarboxylic acid by nitric acid; (2) further oxidative acid treatment of the produced carboxylic acids produces COOH– and OH-coated CDs. Different concentrations of nitric acid was explored to study the effect on fluorescence intensity. It was revealed that a low concentration (0.1 g mL^{-1}) decreased fluorescence while a high concentration (0.2 g mL^{-1}) resulted in a non-fluorescence product. With the concentration of 0.15 g mL^{-1}, the purified product had a size distribution of 6.4 ± 2.7 nm after centrifugation, dialysis, and neutralization processes. The obtained CDs had a broad absorption from 200 nm to 400 nm, with a shoulder around 275 nm. The PL of the CDs showed a prominent emission in the blue–green region with an excitation-dependent feature under 340 nm to 490 nm irradiation. The CDs had a PLQY of 14.6% in methanol and reasonable thermal stability with a PL intensity reduction of 20% at 100 °C. Mondal *et al.* synthesized polyethylene-derived carbon quantum dots (PE-CQDs) with a three-step procedure using H_2SO_4, $KMnO_4$ and H_2O_2 as shown in Fig. 1.[50] Concentrated sulfuric acid was used to melt and char the PE, followed by oxidation with potassium permanganate solution and hydrogen peroxide. The PE-CQDs had a size distribution of 3–10 nm with an average size of 6.5 nm. Dispersion in water and other organic solvents showed a high stability even upon a high-speed centrifugation (40 000 rpm) and no precipitation was observed over two years. The product had an optical absorption edge at 550 nm, with noticeable absorption peaks at 340 nm, 370 nm, 395 nm and 430 nm. The emission of PE-CQDs also exhibited a shift with the excitation wavelength change accordingly from 370 nm to 480 nm. The primary emission was located at a wavelength of 500 nm under 420 nm excitation, with a PLQY of 9.5%. A triple-exponential function accounted for lifetime components of 10.68 ns, 4.15 ns and 0.81 ns, and a mean lifetime of 3.71 ns was fitted for emission under 375 nm pump. The PE-CQDs were able to increase the oxygen content and the ability of O_2 to diffuse in water, thus acting as the catalyst for photocatalytic oxidation reactions. Chaudhary *et al.* also prepared fluorescent CDs from polyethylene bags with a one-step hydrothermal carbonization method.[51] The size distribution confirmed from high-resolution transmission electron microscopy (TEM) was 5–10 nm, while the hydrodynamic diameter is around 27.9 nm. A broad absorption band between 240 nm and 350 nm was observed in the obtained PE-derived CDs, which was assigned to the $n–\pi^*$ and $\pi–\pi^*$ transition of C=C and C=O bonds in CDs.[66] The PL emission intensity was found to increase as excitation wavelength increased from 260 nm to 310 nm, with a PL emission maximum located between 420 nm and 425 nm. However, further increase of excitation wavelength led to a decrease in the emission intensity. Therefore, the PLQY was measured at an excitation wavelength of 310 nm and the value for PP-derived CDs was 62%. This PL emission was attributed to surface emissive traps. To be more specific, the excitons produced at carbogenic cores are easily trapped at the surface defects of functional groups before recombination. It is noted that this synthesis only includes centrifugation and filtration, without a dialysis step to remove molecular impurities and chromo-

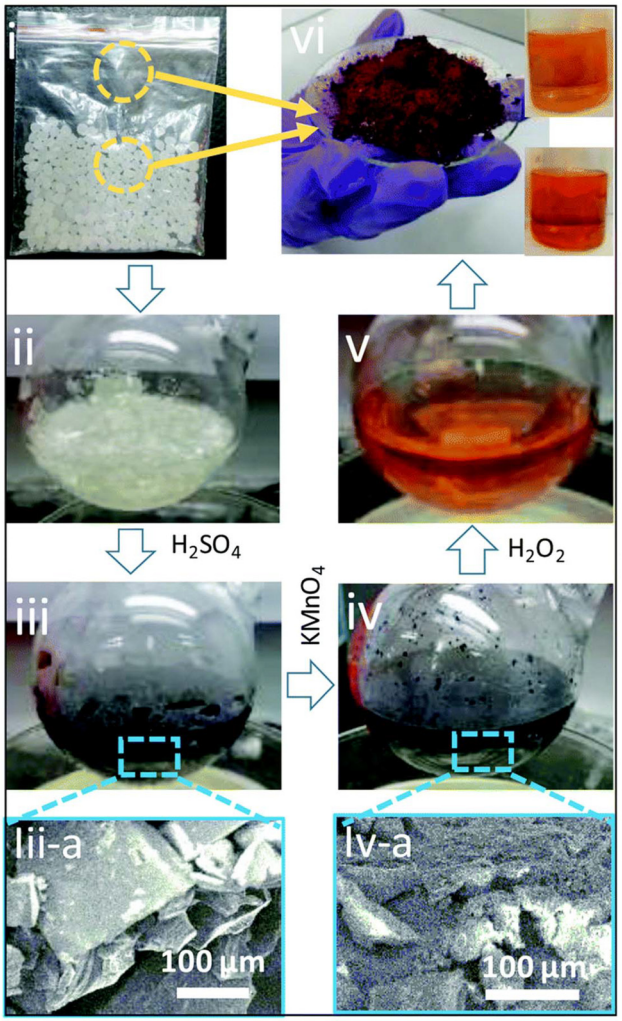

Fig. 1 Photographs showing the transformation from polyethylene into graphitic carbon quantum dots (PE-CQDs). The first step is the acid treatment of PE (i) at ~150 °C leading to swelling (ii) and charring (iii). iii-a shows the SEM image of the charred product containing graphitic sheets. $KMnO_4$ is added in the second step resulting in a stable black dispersion (iv). The oxidation process leads to functionalization of the graphitic sheets creating a rough surface (iv-a). In the final step, hydrogen peroxide is added into the reaction aliquot yielding an orange-yellow colored stable dispersion of PE-CQDs (v). (vi) Photograph of solid PE-CQDs (5.4 g) obtained from 8 g of polyethylene. Inset images show undisturbed, two-year old PE-CQD solutions in water (bottom) and ethyl acetate (top). Reprinted with permission from ref. 50. Copyright 2020 Royal Society of Chemistry.

phores in the system, which may account for the high PLQY. Gautam and co-workers developed a two-step strategy to prepare PE-CQDs, where concentrated sulfuric acid was used as the carbonization reagent and $KMnO_4$ (or H_2O_2, HNO_3, $HClO_4$, and NaClO) was used as the oxidative reagent. The resulting PE-CQDs solution could capture a large amount of molecular O_2 from the air. Density functional theory calculations indicated that the oxygen-trapping capability was related to the surface groups, and was promising for use in photocatalytic reactions.[67,68] Their most recent study indicated that H_2SO_4 can be used for up to 7 cycles in the reactions, further improving the environmental effect of plastic waste upcycling.[69] Looking at the optical properties of PE-derived CDs, it is observed that the emission of CDs prepared from an oxidative synthesis exhibited excitation-dependent behavior, while CDs prepared directly from PE mainly showed an excitation-independent PL emission behavior. Furthermore, sufficient purification steps are necessary to study the PL emission as we noticed large PLQY differences for PE-derived CDs from different preparation methods.

2.2. Polypropylene (PP)

Apart from polyethylene, polypropylene is another heavily used plastic in our daily life. A few groups have also tried to upcycle PP into luminescent CDs with various synthesis procedures. Yang *et al.* prepared CDs from PP with a two-step process, non-solvent induced phase separation and hydrothermal reaction. With the carbonization temperature increases, the obtained CDs exhibited narrower emission distribution in wavelength and higher PLQY. Further Fourier transform infrared spectroscopy (FT-IR) and X-ray photon spectroscopy analysis indicated that it was caused by the more diverse sulfur-related functional groups on the surface and N-doping in the carbon core.[70] Abdelhameed *et al.* also synthesized CDs from PP-based masks, whose consumption increased a lot during the COVID-19 pandemic as shown in Fig. 3(a).[49] A hydrothermal treatment was carried out on PP-based masks under 180 °C with dilute nitric acid and no preprocess mentioned. With the same purification method, the product from PP-based masks showed a smaller size and narrower distribution of 4.5 ± 1.7 nm. The prepared CDs exhibited similar luminescence behavior compared to that of CDs from PE-based bags with the same synthesis route, while the PLQY is slightly higher, which is 16% in methanol. The aforementioned hydrothermal carbonization method was also applicable to PP-based cups according to Chaudhary, see Fig. 3(b).[51] However, the CDs obtained from PP-cups exhibited a less-obvious relationship between emission intensity and excitation wavelength, with a slightly higher PLQY of 65%, compared to that of CDs from PE-based bags, which was 62%, caused by surface defects and size differences of the formed CDs. Another thermal treatment of PP was reported by Aji *et al.*, see Fig. 2, together with a heating temperature effect study.[52] With the increase of heating treatment temperature from 200 °C to 250 °C and 300 °C, the average size of particles decreased from 15 nm to 8 nm. However, due to insufficient purification steps, all three products had a wide distribution in diameter. The absorbance of the resulting polymer CDs increased significantly when the synthesis temperature was increased, together with a slight redshift of the absorbance peak. The calculated bandgap increased from 2.8 eV for the product from 200 °C, to 3.45 eV for the product from 300 °C. The three polymer CDs exhibited similar emission spectra, while higher temperature products showed a lower luminescence intensity. A two-peak emission was observed in the three products, with two main peaks at

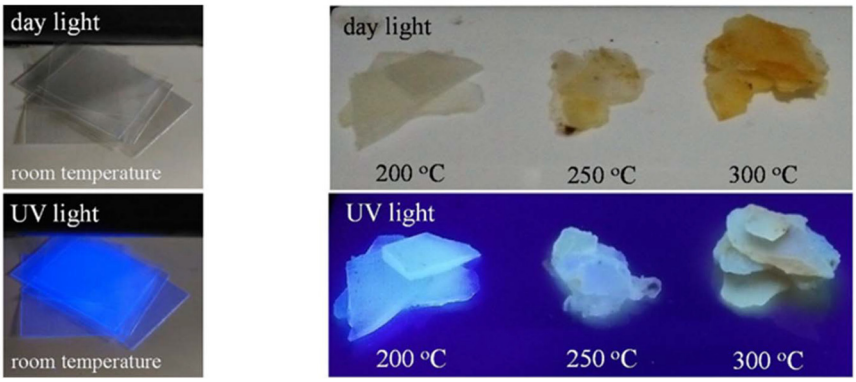

Fig. 2 Left: Pieces of PP plastic waste in daylight (upper-left image) and under UV light (lower-left image). Right: Pieces of heated PP plastic waste in day light (upper-right image) and under UV light (lower-right image). Reprinted with permission from ref. 52. Copyright 2018 Elsevier.

410 nm and 440 nm, and an additional shoulder at 465 nm. It is noted that several reported works applied similar methods to carbonize PP and PE due to the similarity in their backbone structure. The CDs from PP *via* the same approach exhibited slightly higher PLQY in both cases (hydrothermal method and direct heating method). However, more investigation is required to establish the correlation between the precursors and product PL prepared from the same approach.

2.3. Polyolefins

Waste polyolefin (WP) pyrolysis residue has also been processed to prepare green-fluorescent carbon quantum dots (CQDs) using a hydrothermal method, see Fig. 3(c).[53] In the reaction, sulfuric acid and nitric acid were both used as the solvent for the reaction at 120 °C. Purification, including neutralization, filtration and dialysis was employed to remove the unreacted reagents and molecular fluorophores. The prepared CQDs had a relatively narrow size distribution between 1.5 nm and 3.5 nm. A broad absorption between 200 nm and 500 nm with a weak peak around 280 nm was observed in the CQDs, which was assigned to the π–π^* transition. An excitation-dependent fluorescence was observed of the CQDs with primary emission at 540 nm under 490 nm excitation. This emission redshifted as the excitation wavelength increased and this is attributed to the oxygen-containing group on the surface of CQDs. The fluorescence of the product exhibited a pH-dependence and was stable over a period of a month. To be more specific, the fluorescence intensity of the CQDs was increased in presence of acidic medium (pH 2–pH 5), remained almost constant at (pH 6–pH 9), and then decreased in basic (pH 11) medium. The increase in fluorescence intensity at lower pH may be attributed to C=O groups. The presence of a more positive charge on the CQDs can lead to a higher net surface charge that causes electrostatic repulsion, and thus increases PL intensity.

2.4. Polystyrene (PS)

Extended polystyrene is another hydrocarbon thermoplastic that is extensively used in packaging and thermal insulation. Song *et al.* synthesized hydrophobic CDs with a solvothermal method, together with nitric acid as an additional reagent to adjust the optical property of the product, see Fig. 4(a).[54] It was noted that the color of the CDs gradually deepened from light yellow to brown as the amount of nitric acid increased, as well as the average size decreased. The solid powder CDs were obtained after removing the solvents by heating and they were named W-, Y-, and O-CDs based on their colors. These three CDs showed broad absorption at 260 nm and an excitation-dependent emission. The PLQY were 5.2%, 3.4% and 3.1% for solid state W-CDs, Y-CDs and O-CDs, respectively. In particular, the emission of O-CDs in ethanol gradually changed from blue to red wavelengths as the nitric acid concentration increased, which was attributed to resonance energy transfer of O-CD aggregates based on fluorescence microscopy and lifetime studies. Similarly, Ramamurthy and coworkers synthesized highly fluorescent CDs also from expanded polystyrene (EPS) with a solvothermal method, but adding ethylenediamine (EDA) as an extra nitrogen doping source, see Fig. 4(c).[55] The CDs ranging in size from 2.8 nm to 5.2 nm were achieved after several purification procedures of the raw products, including filtration, centrifugation, and dialysis. The UV-visible absorption spectrum of as-prepared CDs extended up to 600 nm without noticeable features. The excitation-wavelength-dependent PL spectra indicated two distinct peaks contributing to emission between 400 nm and 500 nm. It is believed that the first excitation peak centered at 275 nm is from the carbon core and the second peak, which increases from 360 nm to 380 nm, is from surface excitation of functional groups. However, two contours were observed in the 2D fluorescence contour pattern and there was not much difference in the emission centers, which indicates that "even when the excitons are generated from the carbogenic core, they get trapped and relax at the surface defects before recombination".[71,72] The PLQY of the purified product reaches 19.9%, indicating the role of EDA as the surface passivating agent. Huang *et al.* also accidentally synthesized CDs (called WEPSCDs1) from polystyrene using a hydrothermal method.[56] TEM imaging indicated that the product

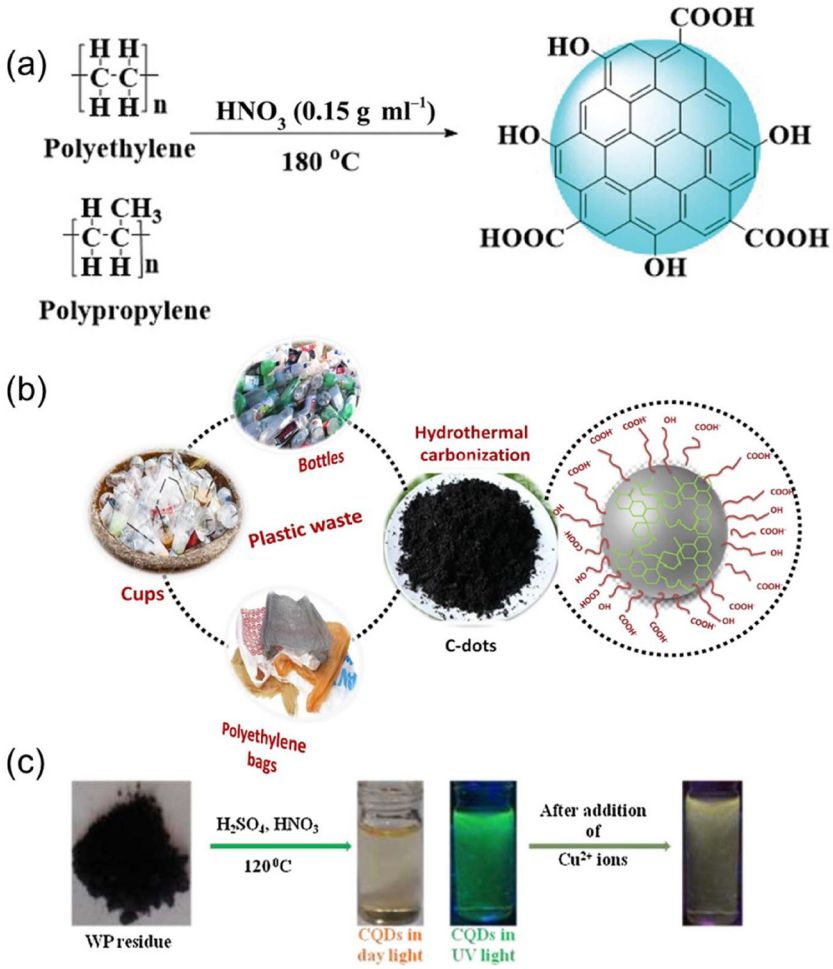

Fig. 3 Schematics of polyolefin-derived CDs. (a) Hydrothermal synthetic route to produce CDs from PE and PP plastics. Reprinted with permission from ref. 49 Copyright 2023 Royal Society of Chemistry. (b) Schematic illustration showing the formation of CDs from three different types of plastic waste by the hydrothermal carbonization method. Reprinted with permission from ref. 51. Copyright 2021 Elsevier. (c) Schematic illustration for the hydrothermal synthesis and sensing application of CQDs from WP residue. Reprinted with permission from ref. 53. Copyright 2018 Elsevier.

assembled into vesicles with single particles less than 10 nm in size as seen in Fig. 4(b). The absorption spectrum of the obtained CDs had a shoulder at 262 nm. The PL emission peak position shifted from 415 to 542 nm as the excitation wavelengths progressively increased from 310 to 470 nm, along with a decrease in emission intensity, which is due to the existence of –OH and –COOH groups as energy traps on the surface of CDs. The PLQY of the CDs is 13.2% under 310 nm excitation. In the above reports, CDs were prepared from PS mainly by solvothermal or hydrothermal methods. It is noted that the oxidation status of CDs and additional heteroatom doping influence the PL emission.

2.5. Polyurethane (PU)

Polyurethane foam is another highly used plastic in a variety of applications. It is promising for producing highly fluorescent CDs due to its high nitrogen and oxygen percentage, which is consistent with enhanced PL by hetero-atom doping.[73,74] A pyrolysis in sulfuric acid was employed to prepare highly photoluminescent CDs with optimization of acid concentration, heating temperature and time both by simulation and experiment, see Fig. 5.[57] The simulation was carried out using a Box-Behnken design response surface methodology (RSM) run on Design Expert V.7. RSM is a powerful tool that combines mathematical and statistical protocols for designing experimental conditions and quantifying relationship between input factors and responses. Among all factors, temperature was found to be the most important parameter affecting the PLQY of the CDs. 300 °C was too high to prepare a highly fluorescent product; if combined with a high acid concentration or long reaction time, the PLQY of the product was lower than 5%, indicated in both experiment and calculations. The calculated condition that gives the highest PLQY of 25.4% is 3.0 M H_2SO_4, 200 °C and 4 h, while the experiment achieved a QY of 33%. The CDs obtained showed a strong absorption between 200 nm and 500 nm, with two shoulders at 250 nm and 300 nm. The emission of the CDs exhibited an excitation-independent feature with the emission

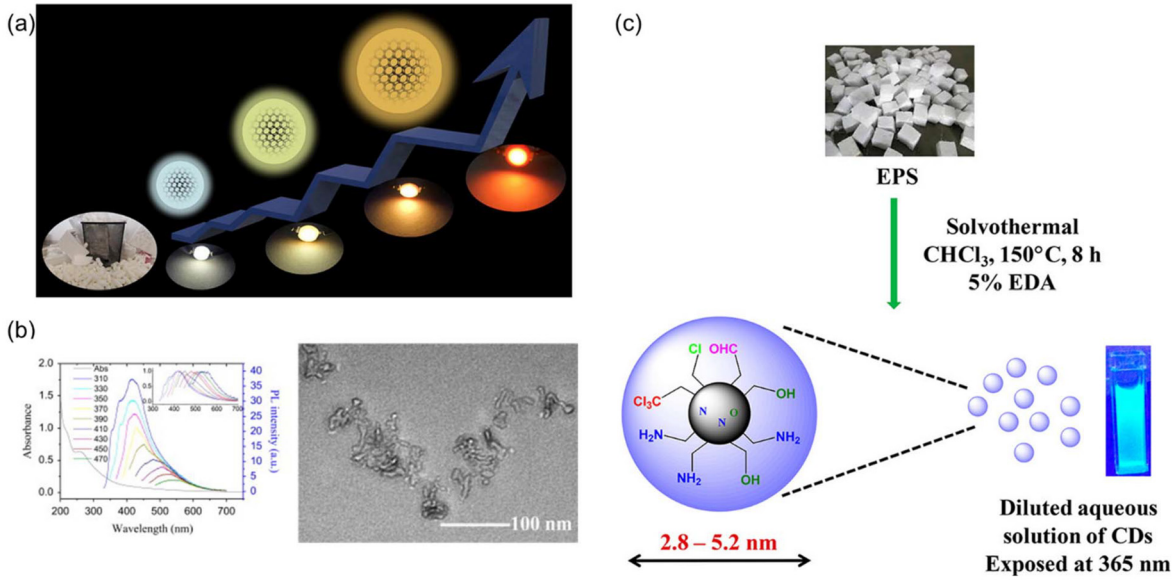

Fig. 4 Schematics of PS-derived CDs. (a) Schematic of the fabrication of solid-state fluorescent CDs with tunable emission prepared from solvothermal reactions. Reprinted with permission from ref. 54. Copyright 2019 Elsevier. (b) Left: Emission spectra of WEPSCDs1 at different excitation wavelengths with a 20 nm increment. Inset: Normalized emission spectra. Right: TEM image of the WEPSCDs1 in water solution. Reprinted with permission from ref. 56. Copyright 2014 Elsevier. (c) Schematic diagram of the synthesis of luminescent CDs from waste EPS. The particles have a diameter from 2.8 nm to 5.2 nm, with amide, hydroxyl, aldehyde and trichloromethyl groups observed on the surface. Reprinted with permission from ref. 55. Copyright 2018 American Chemical Society.

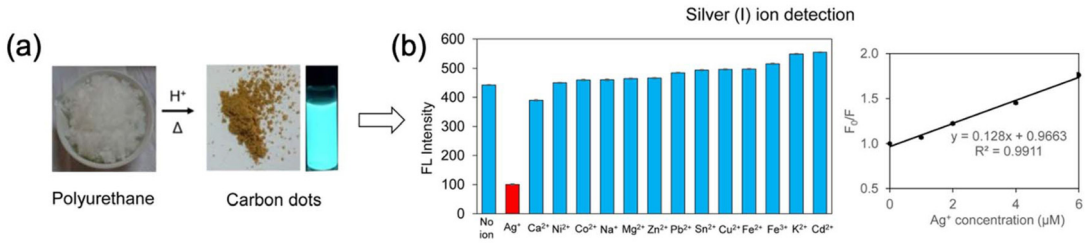

Fig. 5 (a) Synthesis of CDs from polyurethane foam using a one-step pyrolysis method, and (b) their sensing application for silver ion detection. Reprinted with permission from ref. 57. Copyright 2019, Elsevier.

peak centering around 490 nm. It is noted that molecular fluorophores and large particles were removed in the product by a dialysis step. Therefore, the high PLQY (33%) was attributed to the high nitrogen (5.1%) and sulfur (4.8%) content and increased conjugation in the CDs core based on the excitation-independent emission feature.

2.6. Polyethylene terephthalate (PET)

Plastic bottles, which are mainly composed of polyethylene terephthalate, have also accumulated to a considerable problem. Therefore, upcycling PET has recently become an emerging field. Potential functional products include construction and composite materials, oil spill adsorbents, sound isolation aerogels, hydrogel adsorbents for water cleaning, and benzoxazine resins for encapsulants. Hu *et al.* synthesized CDs from PET with a two-step process, air oxidation and the hydrothermal method with H_2O_2 as oxidative reagent, see Fig. 6(a).[60] Centrifugation and dialysis were carried out to purify the raw product. The obtained CDs exhibited a broad absorption around 270 nm, which was assigned to the n–π* transition. The excitation-dependent behavior indicated that the PL was caused by emissive surface traps as well as the wide distribution of the particle sizes. The PLQY of the CDs was 5.2%, which was higher than the CDs prepared from waste plastic bags with a similar pathway.[75] This can be attributed to the diversity of elements in PET compared to that of PE-based bags. Kayee Chan *et al.* explored several reaction pathways of converting PET into CDs to study the influence on luminescence properties.[58] A direct hydrothermal conversion and a combination of pre-treatment including pyrolysis, glycolysis and aminolysis, and a following hydrothermal reaction were studied as shown in Fig. 6(b). A dialysis with cutoff of 2 kDa was employed to purify the raw product. They found that the

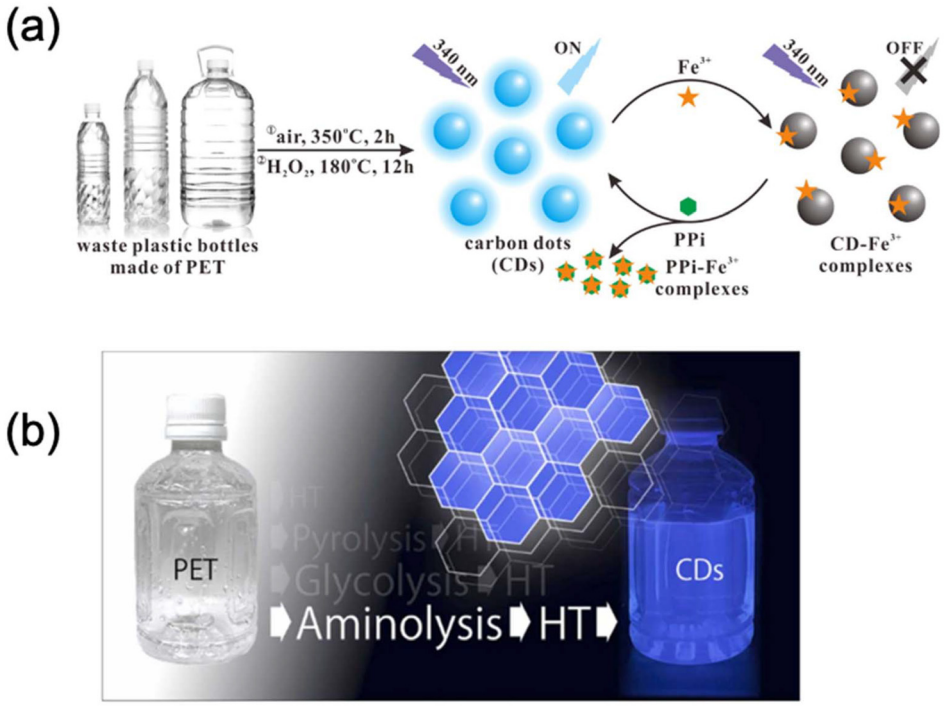

Fig. 6 (a) Schematic showing the green and low-cost synthesis of fluorescent CDs by a two-step process of air oxidation and hydrothermal reaction from waste PET and their use for "on–off–on" sensing of ferric and pyrophosphate ions by an electron transfer mechanism. Reprinted with permission from ref. 60. Copyright 2019 Elsevier. (b) Schematic of fluorescent PET-derived CDs with different preprocess approaches. Reprinted with permission from ref. 58. Copyright 2022 Elsevier.

CDs produced (called PD-NCDs) from the combination of an aminolysis with diethylenetriamine and a hydrothermal reaction with H_2O_2 exhibited enhanced fluorescence (tens to hundreds-fold higher luminescence intensity) and higher PLQY of 9.1% compared to other synthesis approaches. Based on their explanation, the improved luminescence was caused by a surface passivation phenomenon, where the surface electrons were trapped by the nitrogen- or oxygen-including functional groups for more efficient radiative recombination and thus enhanced the fluorescence. The presence of pyrrolic–N and pyridinic–N bonds in PD-NCDs implied that N-containing functional groups were incorporated into the sp^2 aromatic carbon structure and enhanced the luminescence. The N-doping enhanced PL phenomenon has been observed in CDs prepared both from polymer and organic molecules precursors.[38,65,76,77] Similarly, Ma *et al.* synthesized CDs from PET and pyromellitic acid dianhydride as precursors, with urea as an additional nitrogen source.[59] The PET first underwent an alcoholysis of ethylene glycol, after which the other two molecules were added to the system and undergo a solvothermal reaction with tetrahydrofuran as the solvent. A filtration of 0.22 μm and dialysis of 2 kDa were employed to purify the raw product. The obtained CDs had a narrow size distribution from 1.6 nm to 2.9 nm and showed excitation-dependent PL with primary emission under 470 nm excitation, with a PLQY of 48.16%. It is noted that there were two emission centers in the nitrogen-doped CDs based on the PL lifetime measurements. The CDs showed great potential in LED devices and in detecting the water percentage in organic solvents based on a dynamic luminescence-quenching mechanism due to the change in PL lifetime.[78] Also, Lisak and coworkers, and Zhang and coworkers synthesized CDs less than 5 nm in diameter from PET with an oxidative hydrothermal route.[79,80] Apart from hydrothermal and solvothermal methods, a direct thermal calcination method was also applicable to upcycle PET to fluorescent CDs as reported by Chaudhary *et al.*[51] The obtained CDs, compared to ones from PE-bags and PP-cups, showed similar excitation-dependent luminescence and comparable PLQY of 64%, which is attributed to both fluorophores and carbon dots in the dispersion. This is complied with the work by Hu *et al.* on PE and PET.[60,75] Compared to other precursors, including polyolefin, PS and PU, PET is more widely studied due to the lower resistance to heat and chemicals. It is also noted that several works applied preprocess steps on PET, including oxidation, alcoholysis and aminolysis with additional reagents to improve the PL of CDs.

2.7. Polyethylene glycol (PEG)

Water-soluble carbon nanodots (CDs) can also be prepared from PEG with a one-pot method, where PEG serves as both carbon source and surface passivating reagent.[9] The product showed good solubility in water and common organic solvents.

The size of the CDs is related to the heating time of PEG, with the size increasing from 2.3 nm to 4.7 nm when heating increased from 0.5 h to 6 h. Though both products exhibited emission red shifts with increasing excitation wavelength, the emission band of the CDs from the 6 h-treatment was broader and more redshifted. A formation mechanism of the product was proposed – starting with chain cleavage and oxidation, followed by generation of carbon radicals and then formation of hydrophobic carbon cores. The PL of the CDs showed high stability over 60 minutes when kept under UV irradiation. The PL lifetime decay profile of the CDs exhibited double-exponential decay kinetics (CDs from 6 h heating showed a τ_1 = 2.57 ns, τ_2 = 9.07 ns), which was attributed to a fast band gap transition and long decay of oxygen-related emission. Different photonic behaviors in solvents with different polarity were also observed due to different aggregation in those solvents caused by the surface groups of the CDs. However, the PLQY of the obtained PEG-derived CDs was low (2% to 4%), which might be attributed to the low reaction temperature, short reaction time and open system.

2.8. Polylactide (PLA)

Lauria *et al*. synthesized luminescent CDs *via* a hydrothermal method from degraded PLA oligomers, see Fig. 7.[61] To prepare N-doped CDs, TTDDA was added to another group of PLA oligomers prior to the hydrothermal reaction. They explored the reaction temperature between 180–240 °C, and the reaction time from 4 h to 120 h. The CDs were predominantly amorphous at the macroscale with a short-range structural order at higher temperature or longer time. The PL of the product showed temperature-dependence within the range tested and PL increased significantly when the reaction time increased from 4 h to 20 h. The N-doped CDs showed a redshifted emission under an excitation wavelength in the UVA region, while the non-doped CDs showed emission under UVC-region excitation, which indicated that the N-doping alters the electronic structure.

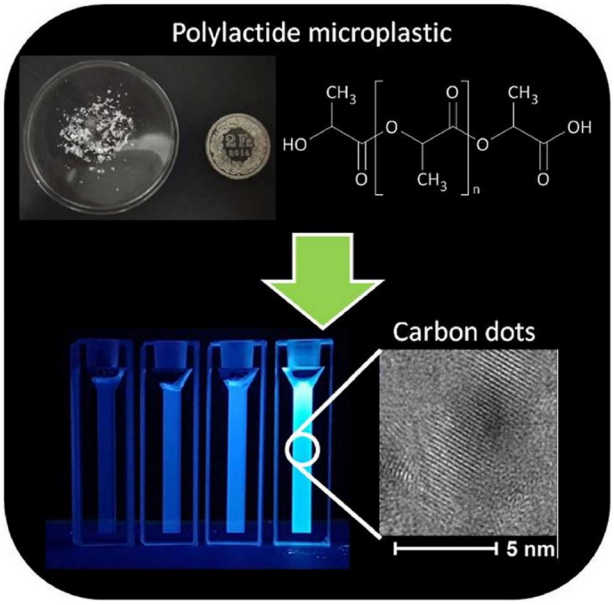

Fig. 7 Illustration of synthesizing fluorescent CDs from PLA with a hydrothermal method, which can be excited with UV light. The crystalline structure of a single CD is shown at the right corner. Reprinted with permission from ref. 61. Copyright 2020 Elsevier.

2.9. Polyacrylamide (PAA)

Zhao *et al*. synthesized N-doped CQDs (N-CQDs) from polyacrylamide as both a carbon and nitrogen source *via* a hydrothermal method. Centrifugation and filtration were employed to purify the raw product. The CDs obtained were uniform in size with an average diameter of 3 nm. They showed good solubility in water and high fluorescence intensity with QY of 23.1%. The N-CQDs could detect dopamine in a basic environment based on fluorescent quenching caused by electron transfer from N-CQDs to dopamine–quinone, which is the oxidative product of dopamine.[62] Tao *et al*. created PAA-derived CDs (called CPDs) by preparing the PAA with acrylic acid (AA) and methylacrylic acid ($AACH_3$). By controlling the ratio of AA and $AACH_3$, three different types of CPDs were prepared with varied number of methyl groups. The prepared CPDs solutions exhibited intense blue fluorescence with an excitation-dependent-behavior. PL lifetime profiles indicated that excess methyl groups lead to a faster decay caused by increased non-radiative pathways (Fig. 8). Furthermore, CPDs powders exhibited significant differences in the afterglow (RTP) when UV illumination was turned off. Structural studies indicated that the extra methyl group caused expanded interplanar spacing and increased spatial hindrance, further leading to energy level changes. Femtosecond transient spectroscopy proved that there were more transition channels in the tight-crosslink CPDs with fewer methyl groups. In this work, the effect of confined-domain CEE on the structure and luminescence properties of CPDs was systematically investigated by combining experimental characterization and theoretical calculations.[46]

2.10. Other natural resources

A wide range of natural resources, including fruit juice, rice, and hair fibers, have been explored to prepare CDs with various methods.[81–83] Bag *et al*. have written reviews to introduce those CDs and their properties.[84,85] Selected examples are included below.

Hu *et al*. synthesized CDs whose emission could be tuned over the whole visible spectrum, from 400 nm to 710 nm from ethylenediamine-end capped polyethyleneimine (PEI), together with citric acid or ethylene glycol.[7] The PL emission under white light excitation was modified by adding a dehydrating reagent (H_3PO_4) or a reducing agent ($NaBH_4$). Detailed characterization revealed that the emission difference was due to the chemical composition difference formed during the dehydration process and the following nucleation and growth process.

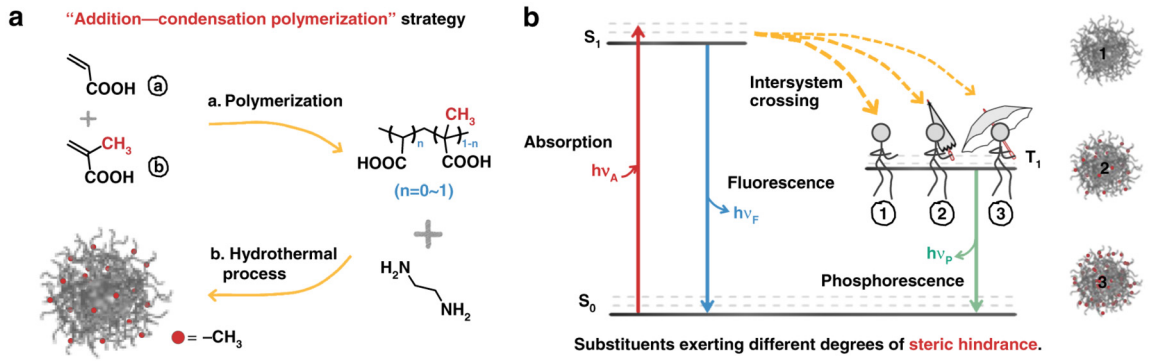

Fig. 8 (a) Schematic of the "addition–condensation polymerization" strategy. (b) Schematic showing a Jablonski diagram of the possible PL mechanism for CPDs with substituents exerting different degrees of steric hindrance (1: no steric hindrance. 2: small steric hindrance. 3: large steric hindrance). Reprinted with permission from ref. 46. Copyright 2022, Crown.

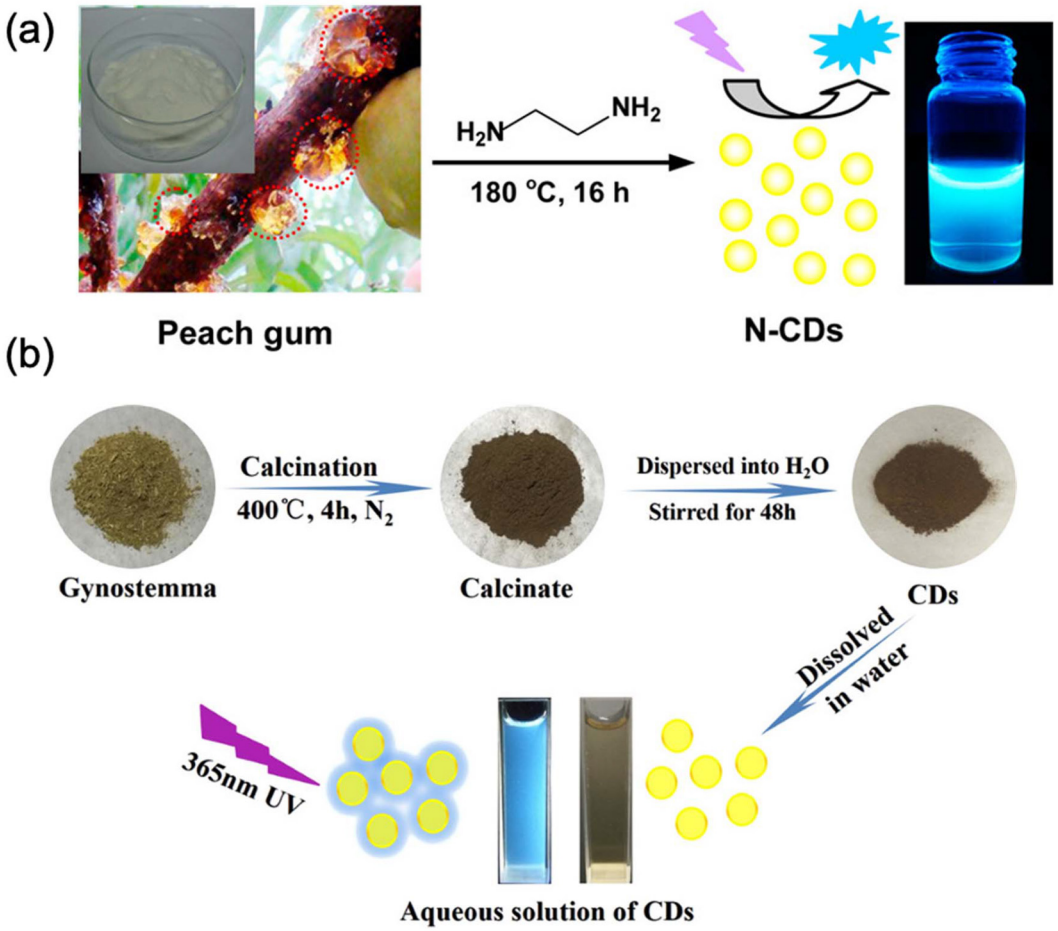

Fig. 9 Schematics of the natural sources derived CDs. (a) Schematic illustration of the preparation of N-CDs from natural peach gum polysaccharide by a one-pot hydrothermal carbonization reaction. Right: Image of N-CDs under a 365 nm UV light stimulation. Reprinted with permission from ref. 63. Copyright 2016 American Chemical Society. (b) Illustration for synthesizing CDs from gynostemma by calcination. The aqueous solution of CDs had a strong absorption in the UV range. Reprinted with permission from ref. 64. Copyright 2019 American Chemical Society.

The final difference was demonstrated in the amount of oxygen-containing and nitrogen-containing groups, which determined the bandgap inside the CDs.

Liao *et al*. synthesized CDs from natural peach gum polysaccharide (PGP) and purified the product with centrifugation and dialysis, see Fig. 9(a).[63] The obtained CDs sized 2–5 nm

with a PLQY of 5.31%. With ethylenediamine as the nitrogen doping source, they found that the PLQY of the nitrogen-doped CDs (N-CDs) reached 28.46%. The study also indicated the high fluorescence stability of the N-CDs against pH and ionic strength change. Fluorescence quenching was observed when mixing the CDs together with Au^{3+} ions caused by the synergistic effects of electron-transfer and fluorescence resonance energy transfer, which resulted indetection with high specificity to the Au^{3+} ion.

Wei *et al.* synthesized fluorescent CDs from gynostemma with a calcination method as shown in Fig. 9(b).[64] The resulting CDs had a narrow size distribution with a mean size of 2.5 nm. The CDs also showed high solubility in water, high fluorescent stability, and good biocompatibility, which made them promising for bioimaging. The CDs could also reduce oxidative damage by controlling reactive oxygen species generation and improving the expression of related antioxidative genes. Therefore, the fluorescent CDs were promising in biomedical applications.

Issa *et al.* synthesized N-CDs from carboxymethylcellulose with the linear polyethyleneimine as the nitrogen source.[65] With the optimization of reaction conditions, the purified N-CDs had sizes ranging from 3 to 8 nm and graphitic cores with the interplanar distance of 0.27 nm. The N-CDs showed the most intense luminescence in water compared to other organic solvents, *i.e.*, acetone and toluene, which may be caused by the photoinduced electron transfer process between intrinsic nitrogen atoms and surface functional groups. The N-CDs could detect Fe^{3+} ions ranging from 0.14–400 μM in an acidic environment by the complexation between the ions and carboxyl and other N-containing function groups as proved by FT-IR.

3. Applications of polymer-derived CDs based on luminescence

3.1. Sensing

Chemical detection is one of the widely used areas for polymer-derived CDs. Both ions and compounds can be detected or measured mostly based on fluorescence quenching mechanisms, including through static quenching, dynamic quenching, Förster resonance energy transfer, photoinduced electron transfer, surface energy transfer, Dexter energy transfer and the inner filter effect. The fluorescence of CDs can be suppressed by quenchers through static quenching, dynamic quenching and different types of energy transfer. Zu *et al.* wrote an overview about different quenching mechanisms in CDs and their applications in detecting and imaging.[78]

3.1.1. Metal ions. Heavy metal ions, including Fe^{3+}, Cu^{2+}, Au^{3+} *etc.*, are common pollutants detected in water, which cause severe environmental and health concerns.[86,87] The fabrication of metal-ion sensors accounts for a large percentage of the research and development into CDs for applications. CDs from carboxymethylcellulose with nitrogen-doping can detect Fe^{3+} ions ranging from 0.14–400 μM in acidic environment by the complexation between the ion and carboxyl and other N-containing groups, which results in a decrease in PL.[65] Compared to CDs used for metal ions sensing that are produced from citric acid and tris(hydroxymethyl)methyl aminomethane and many other natural sources (including bovine serum albumin protein, blueberry and onion waste), the detection range of CDs obtained from carboxymethylcellulose is the widest with the lowest limit of detection (LOD) of 0.14 μM.[88–91] The copper(II) ion is another common target ion for detection due to its essential role in the human body. CDs from pyrolyzed waste polyolefins exhibited good selectivity and sensitivity towards Cu^{2+} detection with a LOD of 6.33 nM.[53] Compared to the up-conversion fluorescence N-doped CDs from citric acid and diethylenetriamine, whose linear detection range is 2.5–50 μM and LOD is 42 nM, the CDs from polyolefins have a smaller detection range of 1–8 μM based on down-conversion fluorescence.[92] CDs from natural PGP and ethylenediamine shows selectivity to Au^{3+} ions with a LOD of 64 nM, while CDs reported from waste expanded polystyrene has a LOD of 53 nM, both of which are higher than the Au^{3+} probe derived from thiourea (29 nM).[55,63,93] The CDs from polyurethane foam show high selectivity towards Ag^{+} ions.[57] The LOD of the obtained CD is 2.8 μM, lower than CDs derived from pectin, but higher than those from citric acid and thiamine hydrochloride.[94,95]

3.1.2. Non-metal ions, pH sensing. Apart from metal-ion sensors, a few CDs exhibited potential for use as pH-sensors. This property is mainly attributed to the protonation and deprotonation of certain functional groups on the surface of CDs, such as –OH, C=O, –COOH. CDs from waste polyolefin pyrolysis residue showed dependence on a wide range of pH values. To be more specific, the fluorescence intensity of the CDs increased in the presence of an acidic medium, remained almost constant in a neutral medium and then decreased in a basic medium. The CD exhibited distinct behavior in the acidic and basic pH ranges, which indicates that CDs have potential as pH sensors. However, more detailed pH-dependent PL studies are required to further develop a pH sensor.[53] In comparison, CDs derived from small organic molecules showed reliable pH-dependent PL. Zhang *et al.* synthesized N- and S-doped CDs from L-cysteine, ethanol and *o*-phenylenediamine, which indicated a distinct pH-sensitive feature with reversible fluorescence and a good linear relationship with pH values in the range of 1.0 to 13.0.[96]

3.1.3. Compound sensing. CDs from polyacrylamide are capable of dopamine detection under basic conditions, where dopamine is oxidized to dopamine–quinone, see Fig. 10(a).[62] Furthermore, the quinone product can accept electrons from CDs and lead to fluorescence quenching. Another strategy to realize compound sensing is *via* an indirect approach. Purbia *et al.* synthesized CDs from coconut water by a microwave-assisted hydrothermal method. They observed both amorphous regions and lattice fringes in an individual carbon dot. The luminescence of the CDs was quenched by Cu^{2+} by

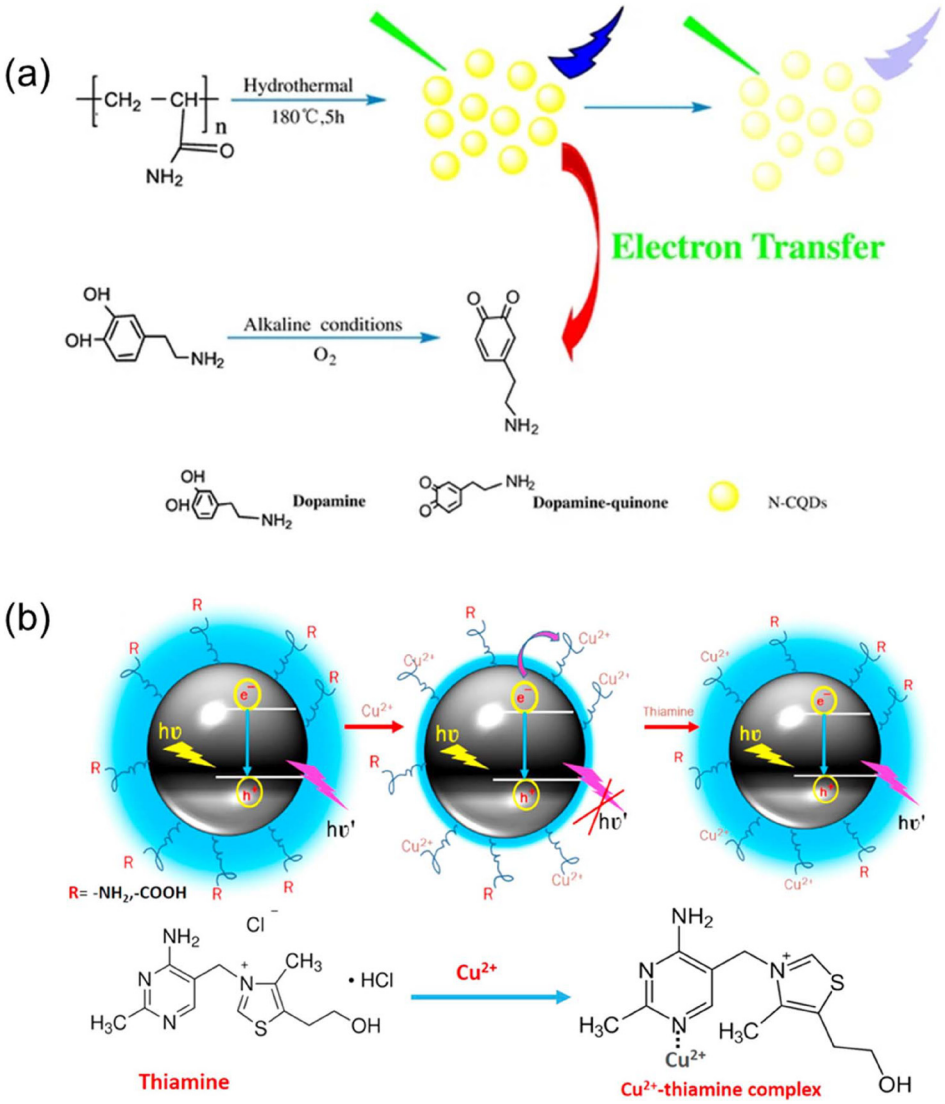

Fig. 10 (a) Scheme of the hydrothermal synthetic strategy for the N-CQDs and the principle of fluorescence quenching. Reprinted with permission from ref. 62. Copyright 2018 Springer Nature. (b) Schematic illustration of the fluorescence response of C-dots in the presence of Cu^{2+} and thiamine. The fluorescence of CDs can be quenched by Cu^{2+} and further recovered by adding thiamine due to the formed complex as indicated in the bottom part. Reprinted with permission from ref. 97. Copyright 2016 Elsevier.

forming a charge-transfer complex and recovered by adding thiamine as it has higher affinity to form a complex with Cu^{2+}, and thus make the CDs free from combination, see Fig. 10(b).[97] This phenomenon can be used to detect thiamine in certain biological environments and the LOD with this method was calculated to be 280 nM.

3.2. Light-emitting diodes

Studies on CD-based LEDs have drawn increasing attention in recent years due to the development of CDs with stable luminescence and high quantum yield. The role of CDs in such LED devices can be categorized into two types: emissive layer and interface transport layer. It is noted that most CDs in such systems are derived from organic molecules, such as citric acid, urea, and diaminonaphthalene because of the tunability of the luminescence wavelengths. Few polymer-derived CDs also show the possibility of being applied in fabricating LED. Ma *et al.* dispersed N-doped CDs derived from PET in PMMA and further coated it on 365 nm and 430 nm LED chips to obtain yellow-light and white-light LEDs as seen in Fig. 11.[59] However, due to the aggregation-induced-quenching (AIQ) effect in CDs, the maximum brightness of CD-based electroluminescent LEDs with pure CDs as the emissive layer is lower than 150 cd m^{-2}, which is far from that needed for many practical applications.[98] Therefore, it is necessary to overcome AIQ effects of CDs presented in the solid-state for incorporation into optoelectronic devices.[99] Chen *et al.* have found that with the introduction of a non-graphitizing polyvinyl alcohol (PVA) chain, on the surface of CDs can prevent the π–π stacking of carbon cores and, therefore, decreases the AIQ effect.[100]

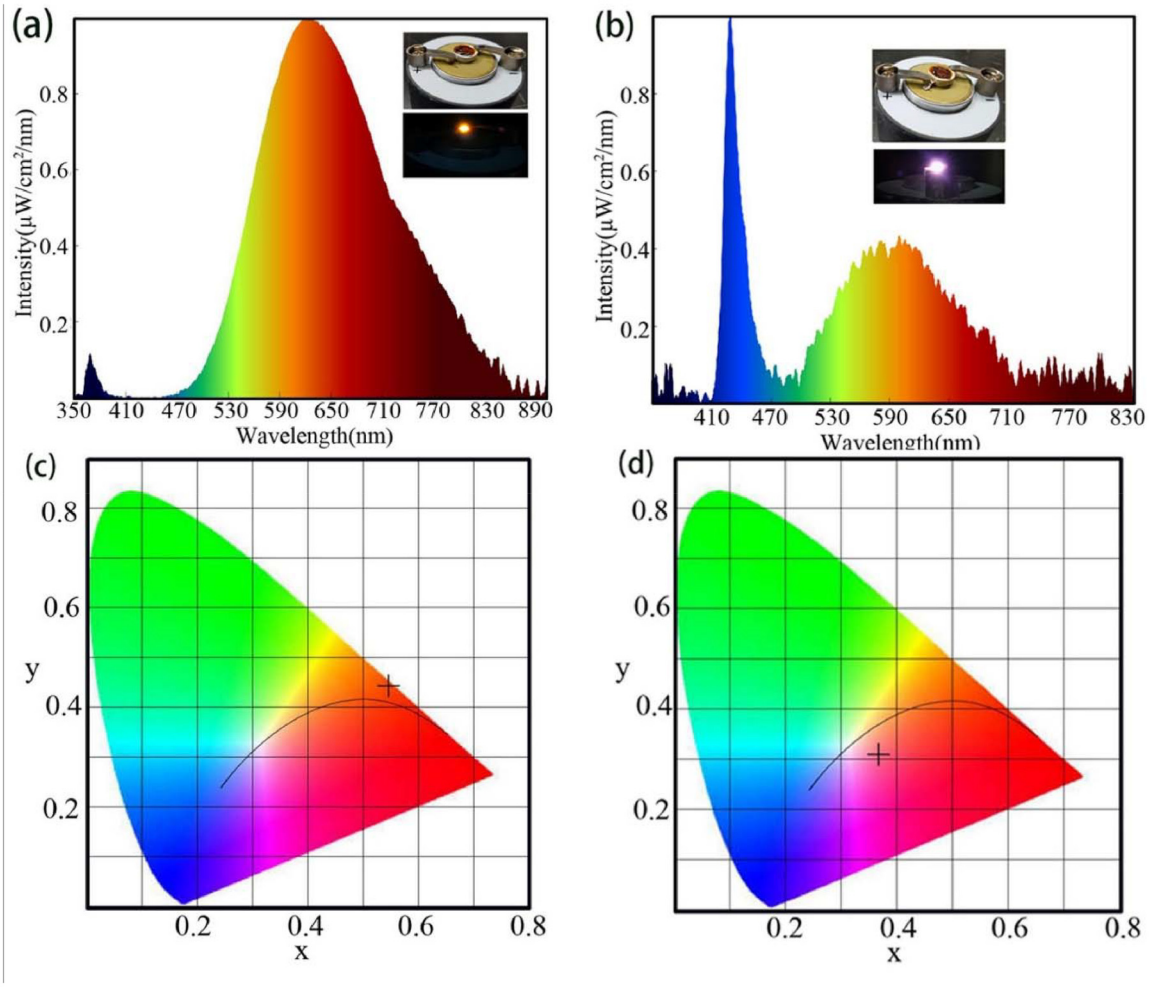

Fig. 11 Emission spectra and images of devices assembled with N-CDs dispersed in a PMMA matrix on LED chips emitting at (a) 365 nm and (b) and 430 nm. Color coordinates of N-CDs dispersed in a PMMA matrix on LED chips emitting at (c) 365 nm and (d) 430 nm (CIE 1931). Reprinted with permission from ref. 59. Copyright 2023 Elsevier.

Shao *et al*. also prepared CDs from maleic acid (MA) and EDA to form a polymer-like structure, which then crosslinked to form solid-state fluorescent polymer carbon dots (SSFPCDs), maintaining an inner polymer core with a net structure.[101] By dispersing SSFPCDs solution in a starch matrix to form a composite, solid-state LEDs with luminescence from red to blue can be obtained due to a concentration-dependent emission. However, most polymer-derived CDs have not realized emission in the red wavelength region. Compared to the high PLQY of 86% and the maximum luminance of 5248–5909 cd m^{-2} of red-emissive, electron-donating-group-passivated CQDs derived from the small molecule, phenylenediamine,[102] optimizing the synthesis of CDs from polymer precursors still requires more exploration.

3.3. Bioimaging

Due to the low toxicity and stable luminescence, applying CDs in bioimaging is widely studied. CDs derived from gynostemma were applied in transparent zebrafish embryos for *in vivo* imaging as indicated in Fig. 12.[64] An intense fluorescence was observed after a 22-hour incubation. Liao *et al*. proved that CDs from peach gum polysaccharide can also realize high-intensity and stable fluorescence after incubation with MCF-7 breast cancer cells, with a low cytotoxicity (90% survival rate within 24 h).[63] Similarly, CDs from polyolefins also show the potential for analysis in triple negative cancer cells.[53] Chen *et al*. indicated that CDs from PEG act as a good cell imaging alternative, which only entered the endocytosis of HeLa cells without penetration into the nuclei.[9]

3.4. Anti-counterfeiting/fluorescent inks

Guo *et al*. synthesized CDs with a PLQY of 45% from Turtle shells using a pyrolysis approach.[103] The CDs served as an ink to print different fluorescent patterns, which exhibited a single-signal anti-counterfeiting function as shown in Fig. 13. Furthermore, the CDs, together with carboxyl group-tailored microspheres, can be used to prepare a nanocomposite with collective optical properties for 3D microflui-

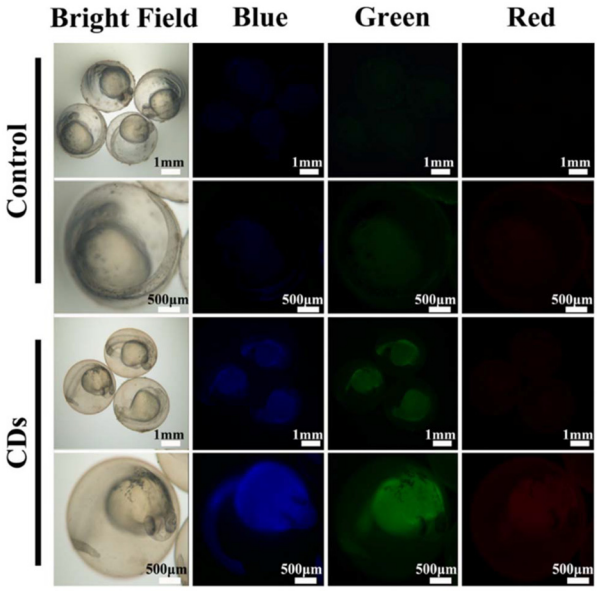

Fig. 12 Example of CDs for bioimaging applications. Fluorescent images of 2 h post-fertilization embryos incubated in CDs solution (400 μg mL^{-1}) obtained by a fluorescence microscope under different excitation wavelengths. Reprinted with permission from ref. 64. Copyright 2019 American Chemical Society.

dic printing. Compared with CDs synthesized from citric acid and urea with a similar function, the PLQY of CDs from Turtle shells was much lower.[104] However, both CDs need to incorporate other fluorescent species for multicolored anti-counterfeiting code applications due to the single emission around 520 nm.

4. Perspectives of polymer-derived CDs

4.1. Synthesis and purification approach

Conversion of polymers into CDs is an emerging area of research with a wide variety in both starting materials and reaction pathways. In this review, we focused on the correlation between synthesis and optical properties of polymer-derived CDs. However, it is noted that there is not a standardized reaction recipe for CDs even within a specific polymer class. Hydrothermal and solvothermal methods are the most commonly used synthesis methods due to the ability to employ high temperature and high pressure at the same time. While the optimal carbonization temperature varies from reaction to reaction, it is apparent that temperature is the most important factor in determining the luminescence properties of the product, as indicated by several studies. A higher reaction temperature often leads to a smaller particle size and a narrower size distribution in such syntheses. It is noted that in a hydrothermal reaction, a mid-range temperature (usually 180 °C to 200 °C) will lead to an increase in luminescence intensity, while a much higher temperature (normally >220 °C) leads to excessive carbonization and quenching of the luminescence. In terms of purifying the raw product, a large percentage of reports employ a combination of centrifugation, filtration and dialysis, though experimental details vary. However, it is necessary to mention that dialysis is important to rule out contributions to CD fluorescence from molecular chromophores produced as byproducts during CDs synthesis. In certain cases, an alcohol extraction or wash can be considered as a replacement for dialysis.

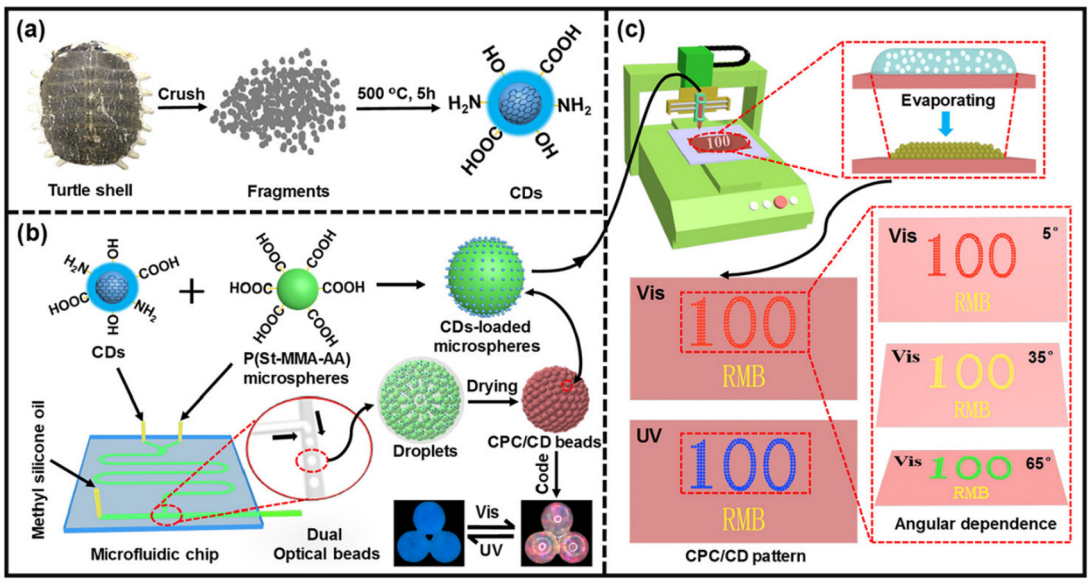

Fig. 13 Example of CDs for anti-counterfeiting applications. (a) Schematic of the preparation of CDs *via* pyrolysis of turtle shells. (b) Schematic of the assembly of CD-loaded microspheres and the formation of hybrid bead codes with structural color and fluorescence *via* a microfluidic device. (c) Construction of multi-signal anti-counterfeiting patterned films with fluorescence and angular dependence of structural colors *via* a 3D microfluidic printing technique. Reprinted with permission from ref. 103. Copyright 2020 American Chemical Society.

4.2. Optical properties and data interpretation

Table 1 summarizes the synthesis methods and optical properties (absorption, emission mechanism and PLQY) for different polymer-derived CDs. Synthesis methods vary, with the most common being hydrothermal due to its ability to effectively carbonize the polymer, while adding functional groups or dopants during the synthesis. It is also apparent that most CDs have an absorption tail from 200 nm to 400 nm, with a peak usually observed between 250 nm and 280 nm, which is assigned to n–π* transition, see Fig. 4(b) for example. The vast majority of polymer-derived CDs exhibit excitation-dependent emission, likely due to either presence of fluorophores and/or emission that is influenced by the functional-group(s). The PLQY values vary substantially across the range of polymer-derived CDs, and, even for the same precursor, the PLQY can be lower than 10% or greater than 40% (see PLQY values for PET in Table 1, for example). Though polymer-derived CDs have been applied in several fields based on their PL properties, as discussed, few mechanism studies have been carried out, especially on the origin of the PL. Transient PL lifetime measurements are helpful to differentiate the quenching mechanism in some cases by a Stern Volmer (SV) plot, *e.g.*, a linear relationship in the SV plot indicates dynamic quenching. However, due to the complexity of the system, it is challenging to deconvolute the lifetime decay species and assign to specific pathways. Performing theoretical calculations on these CDs, *e.g.*, to determine frontier orbital energies and bandgaps, can also be challenging considering the variations in particle sizes and uniformity. Instead, an estimation of the bandgap from the Tauc equation applied to absorption spectra was employed in several reports. The applicability of the Tauc plot requires no secondary absorption in the system, while CDs usually have several absorption and emission origins. Though transient spectroscopy has been widely applied to analyzing the excited states of molecule-derived CDs, it is rarely employed in the study of polymer-derived CDs due to the complexity of the products.[105] Transient spectroscopy could be a powerful tool to obtain insight into the fundamental PL origin of the polymer-derived CD system if carried out with appropriate purification procedures and test/control sample preparation.

Additional nitrogen-containing chemicals, such as EDA, are used as surface-passivating reagents in some syntheses. Several studies have shown that nitrogen-doping can enhance the PL intensity and increase the PLQY of CDs, mostly due to the increased surface emissive traps. Similarly, oxidative reagents, such as H_2O_2 and HNO_3, sometimes are also added to the reaction. The amount of those additional oxidants also has an influence on the PL wavelength range and PL intensity of CDs. As the oxidation extent increases, the bandgap decreases, and a redshifted emission is observed in several

Table 1 Summary of the optical properties of polymer-derived CDs

Precursors	Synthesis method	Absorption region	Emission mechanism	PLQY
PE	Oxidation-hydrothermal[49]	200–400 nm	Excitation-dependent	14.6%
	Doped hydrothermal[50]	350 nm	Excitation-dependent	9.5%
	Thermal calcination[51]	240–350 nm	Excitation-dependent	62%[a]
PP	Oxidation-hydrothermal[49]	200–550 nm	Excitation-dependent	16%
	Heat treatment[52]	420 nm	Stimulated emission	—
	Thermal calcination[51]	240–350 nm	Excitation-dependent	65%[a]
Polyolefins	Pyrolysis-hydrothermal[53]	280 nm	Excitation-dependent	—
PS	Solvothermal[54]	260 nm	Resonance energy transfer, excitation-dependent	3.1–5.2%
	Doped solvothermal[55]	200–500 nm	Excitation-dependent, 2 excitation peaks	19.9%
	Hydrothermal[56]	260 nm	Excitation-dependent	13.2%
PU	Pyrolysis[57]	250 nm, 300 nm	Excitation-independent	33%
PET	Aminolysis-hydrothermal[58]	288 nm and 313 nm	Excitation-independent	9.1%
	Alcoholysis-hydrothermal[59]	260 nm	Excitation-dependent	48.16%
	Oxidation-hydrothermal[60]	200–400 nm	Excitation-dependent	5.2%
	Thermal calcination[51]	240–350 nm	Excitation-dependent	64%[a]
PEG	Thermal treatment 0.5 h[9]	246 nm, 310 nm	Excitation-dependent	2.51%
	Thermal treatment 6 h[9]	246 nm	Excitation-dependent	3.58%
PLA	Hydrothermal[61]	275 nm	Excitation-dependent, (primary emission at 318 nm)	—
	Additional N-doping[61]	265 nm	Excitation-dependent, (primary emission at 370 nm)	—
PAA	Hydrothermal[62]	290 nm	Excitation-dependent	23.1%[a]
	Hydrothermal[46]	334 nm	Excitation-dependent	3.13–27.32%
PEI	Heated treatment[7]	300–400 nm	Excitation-dependent	6%–20%
PGP	Doped hydrothermal[63]	274 nm and 350 nm	Excitation-dependent	5.31%
Gynostemma	Thermal calcination[64]	268 nm	Excitation-dependent	5.7%[a]
Carboxymethyl cellulose	Doped hydrothermal[65]	350 nm	Solvent polarity-dependent	20.58%

[a] CDs with no dialysis or solvent wash procedure.

reports. The size of the CDs can also be affected by this factor. In this way, polyesters, in principle, are more promising for preparing CDs with high PLQY due to the variety of constituent elements.

4.3. Comparison with molecule-derived CDs

Compared with CDs derived from small molecules, polymer-derived CDs usually exhibit broader emission spectra and lower PLQY. Up-conversion fluorescence from polymer-derived CDs has not been observed thus far, though it has been demonstrated for CDs derived from citric acid and urea. The emission bandwidth can be understood by considering the different reaction pathways. Though condensation–carbonization happens in both scenarios, polymer precursors are decomposed into monomers and oligomers in the first step, while small molecules themselves act as the monomer with crosslinker compounds added. The ratio of the monomer and crosslinker is more controllable. Therefore, small molecule-derived CDs are more uniform in size and structure, making them more promising for high-performance light-emitting device applications, as they have better tunability of the emission wavelengths and increased PLQY. However, polymer-derived CDs are more promising in the case of a requirement for broader optical absorption. Furthermore, using waste polymer materials as starting reagents to make CDs is a promising approach to repurpose post-consumer plastics that would otherwise be disposed of. It is also observed that some synthetic approaches are feasible for daily waste even without pre-processing or cleaning of the waste plastics. With the emerging interest in the crosslink-enhanced emission effect, researchers are taking advantage of both molecule-derived CDs and polymeric structures to realize emission over the full-color range and to demonstrate afterglow RTP.[106,107]

In conclusion, polymers are promising starting materials to prepare CDs due to the high carbon percentage and large feedstock. The reaction conditions, including concentration, temperature, time, and additional reagents have significant influence on the structure and optical properties of polymer-derived CDs. Reaction simulations may be employed to explore the optimal recipe for specific target properties before carrying out the experiments. To-date polymer-derived CDs still have limited applications in imaging and LEDs due to their low luminescence intensity and light conversion efficiency. Improved synthesis approaches should aim at producing narrow-size-distributions, high PLQY and stable CDs in the future. Synthesizing CDs with increased carbon core density is another promising direction to expand the applications by providing a phosphorescence decay pathway. Developing generalizable synthesis approaches, together with tunable product structures and optical properties is a future direction for research on polymer-derived CDs.

Conflicts of interest

There are no conflicts of interest to declare.

Data availability

No primary research results, software or code have been included and no new data were generated or analyzed as part of this review. The figures were reproduced with permission from the sources specified in the caption of each figure.

Acknowledgements

The authors acknowledge partial support from a Zhou Family Fellowship from the Department of Chemistry and Chemical Biology at Rutgers University, and the US National Science Foundation (2444249).

References

1 H. Zhang, Y. Yang, D. Ren, L. Wang and X. He, *Energy Storage Mater.*, 2021, **36**, 147–170.
2 K. Y. Yasoda, S. Kumar, M. S. Kumar, K. Ghosh and S. K. Batabyal, *Mater. Today Chem.*, 2021, **19**, 100394.
3 S. Khodabakhshi, P. F. Fulvio and E. Andreoli, *Carbon*, 2020, **162**, 604–649.
4 C. Ma, L. Wu, M. Dirican, H. Cheng, J. Li, Y. Song, J. Shi and X. Zhang, *Appl. Surf. Sci.*, 2021, **537**, 147914.
5 X. Xu, R. Ray, Y. Gu, H. J. Ploehn, L. Gearheart, K. Raker and W. A. Scrivens, *J. Am. Chem. Soc.*, 2004, **126**, 12736–12737.
6 F. Yuan, Z. Wang, X. Li, Y. Li, Z. Tan, L. Fan and S. Yang, *Adv. Mater.*, 2017, **29**, 1604436.
7 S. Hu, A. Trinchi, P. Atkin and I. Cole, *Angew. Chem., Int. Ed.*, 2015, **54**, 2970–2974.
8 S. Zhu, Q. Meng, L. Wang, J. Zhang, Y. Song, H. Jin, K. Zhang, H. Sun, H. Wang and B. Yang, *Angew. Chem., Int. Ed.*, 2013, **52**, 3953–3957.
9 M. Chen, W. Wang and X. Wu, *J. Mater. Chem. B*, 2014, **2**, 3937–3945.
10 N. Esfandiari, Z. Bagheri, H. Ehtesabi, Z. Fatahi, H. Tavana and H. Latifi, *Heliyon*, 2019, **5**, e02940.
11 N. Javed, Z. Cheng, K. Zhu, R. Crichton, H. Maddali, G. Hall, J. Zhang, J. Li and D. M. O'Carroll, *ACS Appl. Nano Mater.*, 2022, **5**, 11741–11751.
12 Y. Shi, W. Su, F. Yuan, T. Yuan, X. Song, Y. Han, S. Wei, Y. Zhang, Y. Li, X. Li and L. Fan, *Adv. Mater.*, 2023, **35**, 2210699.
13 Y. Liu, S. Roy, S. Sarkar, J. Xu, Y. Zhao and J. Zhang, *Carbon Energy*, 2021, **3**, 795–826.
14 Y. Zhai, B. Zhang, R. Shi, S. Zhang, Y. Liu, B. Wang, K. Zhang, G. I. N. Waterhouse, T. Zhang and S. Lu, *Adv. Energy Mater.*, 2022, **12**, 2103426.
15 C. Rosso, G. Filippini and M. Prato, *ACS Catal.*, 2020, **10**, 8090–8105.
16 W. Gao, J. He, L. Chen, X. Meng, Y. Ma, L. Cheng, K. Tu, X. Gao, C. Liu, M. Zhang, K. Fan, D.-W. Pang and X. Yan, *Nat. Commun.*, 2023, **14**, 160.

17 Y. Yu, Y. Feng, F. Liu, H. Wang, H. Yu, K. Dai, G. Zheng and W. Feng, *Small*, 2023, **19**, 2204365.
18 D. Xu, Q. Lin and H.-T. Chang, *Small Methods*, 2020, **4**, 1900387.
19 H. Li, X. Yan, D. Kong, R. Jin, C. Sun, D. Du, Y. Lin and G. Lu, *Nanoscale Horiz.*, 2020, **5**, 218–234.
20 L. Cui, X. Ren, J. Wang and M. Sun, *Mater. Today Nano*, 2020, **12**, 100091.
21 A. Kaczmarek, J. Hoffman, J. Morgiel, T. Mościcki, L. Stobiński, Z. Szymański and A. Małolepszy, *Materials*, 2021, **14**, 729.
22 F. J. Chao-Mujica, L. Garcia-Hernández, S. Camacho-López, M. Camacho-López, M. A. Camacho-López, D. Reyes Contreras, A. Pérez-Rodríguez, J. P. Peña-Caravaca, A. Páez-Rodríguez, J. G. Darias-Gonzalez, L. Hernandez-Tabares, O. Arias de Fuentes, E. Prokhorov, N. Torres-Figueredo, E. Reguera and L. F. Desdin-García, *J. Appl. Phys.*, 2021, **129**, 163301.
23 S. Zhu, Y. Song, X. Zhao, J. Shao, J. Zhang and B. Yang, *Nano Res.*, 2015, **8**, 355–381.
24 A. Das, I. A. Arefina, D. V. Danilov, A. V. Koroleva, E. V. Zhizhin, P. S. Parfenov, V. A. Kuznetsova, A. O. Ismagilov, A. P. Litvin, A. V. Fedorov, E. V. Ushakova and A. L. Rogach, *Nanoscale*, 2021, **13**, 8058–8066.
25 C. Liu, M. Wen, X. Zhou, X. Huang, S. Zhang and H. Liu, *ACS Sustainable Chem. Eng.*, 2024, **12**, 12354–12364.
26 A. Khan, P. Ezati and J.-W. Rhim, *ACS Appl. Bio Mater.*, 2023, **6**, 1294–1305.
27 J. Schneider, C. J. Reckmeier, Y. Xiong, M. von Seckendorff, A. S. Susha, P. Kasák and A. L. Rogach, *J. Phys. Chem. C*, 2017, **121**, 2014–2022.
28 Z. Wang, B. Yang, Z. Chen, D. Liu, L. Jing, C. Gao, J. Li, Z. He and J. Wang, *ACS Appl. Bio Mater.*, 2020, **3**, 3785–3791.
29 Y. Zheng, D. Yang, X. Wu, H. Yan, Y. Zhao, B. Feng, K. Duan, J. Weng and J. Wang, *RSC Adv.*, 2015, **5**, 90245–90254.
30 X. Sun, W. He and B. Liu, *J. Phys. Chem. C*, 2022, **126**, 3540–3548.
31 L. Ai, Y. Yang, B. Wang, J. Chang, Z. Tang, B. Yang and S. Lu, *Sci. Bull.*, 2021, **66**, 839–856.
32 Z. Gan, H. Xu and Y. Hao, *Nanoscale*, 2016, **8**, 7794–7807.
33 L. Wang, W. Li, L. Yin, Y. Liu, H. Guo, J. Lai, Y. Han, G. Li, M. Li, J. Zhang, R. Vajtai, P. M. Ajayan and M. Wu, *Sci. Adv.*, 2020, **6**, eabb6772.
34 G. Eda, Y.-Y. Lin, C. Mattevi, H. Yamaguchi, H.-A. Chen, I.-S. Chen, C.-W. Chen and M. Chhowalla, *Adv. Mater.*, 2010, **22**, 505–509.
35 A. I. Ekimov, A. L. Efros and A. A. Onushchenko, *Solid State Commun.*, 1985, **56**, 921–924.
36 H. Ding, S.-B. Yu, J.-S. Wei and H.-M. Xiong, *ACS Nano*, 2016, **10**, 484–491.
37 F. Yan, Y. Jiang, X. Sun, Z. Bai, Y. Zhang and X. Zhou, *Mikrochim. Acta*, 2018, **185**, 424.
38 L. Li and T. Dong, *J. Mater. Chem. C*, 2018, **6**, 7944–7970.
39 D. Qu, Z. Sun, M. Zheng, J. Li, Y. Zhang, G. Zhang, H. Zhao, X. Liu and Z. Xie, *Adv. Opt. Mater.*, 2015, **3**, 360–367.
40 H. Ding, L.-W. Cheng, Y.-Y. Ma, J.-L. Kong and H.-M. Xiong, *New J. Chem.*, 2013, **37**, 2515–2520.
41 X. Zhang, Y. Zhang, Y. Wang, S. Kalytchuk, S. V. Kershaw, Y. Wang, P. Wang, T. Zhang, Y. Zhao, H. Zhang, T. Cui, Y. Wang, J. Zhao, W. W. Yu and A. L. Rogach, *ACS Nano*, 2013, **7**, 11234–11241.
42 Y. Xiong, J. Schneider, E. V. Ushakova and A. L. Rogach, *Nano Today*, 2018, **23**, 124–139.
43 S. Zhu, L. Wang, N. Zhou, X. Zhao, Y. Song, S. Maharjan, J. Zhang, L. Lu, H. Wang and B. Yang, *Chem. Commun.*, 2014, **50**, 13845–13848.
44 P. Li and Z. Sun, *Light: Sci. Appl.*, 2022, **11**, 81.
45 C. Zheng, S. Tao, X. Zhao, C. Kang and B. Yang, *Angew. Chem., Int. Ed.*, 2024, **63**, e202408516.
46 S. Tao, C. Zhou, C. Kang, S. Zhu, T. Feng, S.-T. Zhang, Z. Ding, C. Zheng, C. Xia and B. Yang, *Light: Sci. Appl.*, 2022, **11**, 56.
47 X. He, W. Huang, Y. Zheng, X. Xu, H. Wei, P. Liang, X. Yang, C. Hu, X. Zhang, B. Lei, X. Zhang, J. Ye, Y. Liu and J. Zhuang, *Angew. Chem., Int. Ed.*, 2025, **64**, e202423388.
48 L. Guo, J. Ge, W. Liu, G. Niu, Q. Jia, H. Wang and P. Wang, *Nanoscale*, 2015, **8**, 729–734.
49 M. Abdelhameed, M. Elbeh, N. S. Baban, L. Pereira, J. Matula, Y.-A. Song and K. B. Ramadi, *Green Chem.*, 2023, **25**, 1925–1937.
50 S. Mondal, P. E. Karthik, L. Sahoo, K. Chatterjee, M. Sathish and U. K. Gautam, *Nanoscale*, 2020, **12**, 10480–10490.
51 S. Chaudhary, M. Kumari, P. Chauhan and G. Ram Chaudhary, *Waste Manage.*, 2021, **120**, 675–686.
52 M. P. Aji, A. L. Wati, A. Priyanto, J. Karunawan, B. W. Nuryadin, E. Wibowo, P. Marwoto and S. Sulhadi, *Environ. Nanotechnol., Monit. Manage.*, 2018, **9**, 136–140.
53 A. Kumari, A. Kumar, S. K. Sahu and S. Kumar, *Sens. Actuators, B*, 2018, **254**, 197–205.
54 H. Song, X. Liu, B. Wang, Z. Tang and S. Lu, *Sci. Bull.*, 2019, **64**, 1788–1794.
55 V. Ramanan, B. Siddaiah, K. Raji and P. Ramamurthy, *ACS Sustainable Chem. Eng.*, 2018, **6**, 1627–1638.
56 J. Huang, X.-Y. Yin, J.-Y. Yang and M.-L. Guo, *Mater. Lett.*, 2014, **117**, 112–115.
57 M. I. S. Dela Cruz, N. Thongsai, M. D. G. de Luna, I. In and P. Paoprasert, *Colloids Surf., A*, 2019, **568**, 184–194.
58 K. Chan and A. Zinchenko, *J. Environ. Chem. Eng.*, 2022, **10**, 107749.
59 G. Ma, R. Wang, M. Zhang, Z. Dong, A. Zhang, M. Qu, L. Gao, Y. Wei and J. Wei, *Spectrochim. Acta, Part A*, 2023, **289**, 122178.
60 Y. Hu, Z. Gao, J. Yang, H. Chen and L. Han, *J. Colloid Interface Sci.*, 2019, **538**, 481–488.
61 A. Lauria and E. Lizundia, *J. Cleaner Prod.*, 2020, **262**, 121288.

62 C. Zhao, Y. Jiao, J. Hua, J. Yang and Y. Yang, *J. Fluoresc.*, 2018, **28**, 269–276.
63 J. Liao, Z. Cheng and L. Zhou, *ACS Sustainable Chem. Eng.*, 2016, **4**, 3053–3061.
64 X. Wei, L. Li, J. Liu, L. Yu, H. Li, F. Cheng, X. Yi, J. He and B. Li, *ACS Appl. Mater. Interfaces*, 2019, **11**, 9832–9840.
65 M. A. Issa, Z. Z. Abidin, S. Sobri, S. A. Rashid, M. A. Mahdi and N. A. Ibrahim, *Sci. Rep.*, 2020, **10**, 11710.
66 S. Chaudhary, S. Kumar, B. Kaur and S. K. Mehta, *RSC Adv.*, 2016, **6**, 90526–90536.
67 S. Mondal, S. R. Das, L. Sahoo, S. Dutta and U. K. Gautam, *J. Am. Chem. Soc.*, 2022, **144**, 2580–2589.
68 B. Kommula, S. Chakraborty, M. Banoo, R. S. Roy, S. Sil, A. Swarnkar, B. Rawat, K. Kailasam and U. K. Gautam, *ACS Appl. Mater. Interfaces*, 2024, **16**, 39470–39481.
69 B. Kommula, V. Gehlot, K. Kanwar, S. Sil, M. Banoo, A. Swarnkar, B. Rawat, K. Kailasam and U. K. Gautam, *Carbon*, 2025, **234**, 119960.
70 Y. Yang, S. Sreekumar, R. V. Chimenti, M. Veksler, K. Song, S. Zhang, D. Rodas, V. Christianson and D. M. O'Carroll, *ACS Mater. Lett.*, 2024, **6**, 1968–1976.
71 V. Ramanan, S. K. Thiyagarajan, K. Raji, R. Suresh, R. Sekar and P. Ramamurthy, *ACS Sustainable Chem. Eng.*, 2016, **4**, 4724–4731.
72 S. K. Thiyagarajan, S. Raghupathy, D. Palanivel, K. Raji and P. Ramamurthy, *Phys. Chem. Chem. Phys.*, 2016, **18**, 12065–12073.
73 S. Miao, K. Liang, J. Zhu, B. Yang, D. Zhao and B. Kong, *Nano Today*, 2020, **33**, 100879.
74 Q. Xu, T. Kuang, Y. Liu, L. Cai, X. Peng, T. S. Sreeprasad, P. Zhao, Z. Yu and N. Li, *J. Mater. Chem. B*, 2016, **4**, 7204–7219.
75 Y. Hu, J. Yang, J. Tian, L. Jia and J.-S. Yu, *RSC Adv.*, 2014, **4**, 47169–47176.
76 X. Zhai, P. Zhang, C. Liu, T. Bai, W. Li, L. Dai and W. Liu, *Chem. Commun.*, 2012, **48**, 7955–7957.
77 M. Yang, B. Li, K. Zhong and Y. Lu, *J. Mater. Sci.*, 2018, **53**, 2424–2433.
78 F. Zu, F. Yan, Z. Bai, J. Xu, Y. Wang, Y. Huang and X. Zhou, *Microchim. Acta*, 2017, **184**, 1899–1914.
79 L. Liang, S. C. Wong and G. Lisak, *Chemosphere*, 2023, **316**, 137868.
80 Y. Hu, M. Li, Z. Gao, L. Wang and J. Zhang, *Catal. Lett.*, 2021, **151**, 2436–2444.
81 S. Sahu, B. Behera, T. K. Maiti and S. Mohapatra, *Chem. Commun.*, 2012, **48**, 8835–8837.
82 D. Sun, R. Ban, P.-H. Zhang, G.-H. Wu, J.-R. Zhang and J.-J. Zhu, *Carbon*, 2013, **64**, 424–434.
83 Q. Hu, M. Chin Paau, Y. Zhang, X. Gong, L. Zhang, D. Lu, Y. Liu, Q. Liu, J. Yao and M. M. F. Choi, *RSC Adv.*, 2014, **4**, 18065–18073.
84 P. Bag, R. K. Maurya, A. Dadwal, M. Sarkar, P. A. Chawla, R. K. Narang and B. Kumar, *ChemistrySelect*, 2021, **6**, 2774–2789.
85 X. Lin, M. Xiong, J. Zhang, C. He, X. Ma, H. Zhang, Y. Kuang, M. Yang and Q. Huang, *Microchem. J.*, 2021, **160**, 105604.
86 J. Briffa, E. Sinagra and R. Blundell, *Heliyon*, 2020, **6**, e04691.
87 A. Badeenezhad, H. Soleimani, S. Shahsavani, I. Parseh, A. Mohammadpour, O. Azadbakht, P. Javanmardi, H. Faraji and K. Babakrpur Nalosi, *Sci. Rep.*, 2023, **13**, 15817.
88 M. Zhou, Z. Zhou, A. Gong, Y. Zhang and Q. Li, *Talanta*, 2015, **143**, 107–113.
89 Q. Yang, L. Wei, X. Zheng and L. Xiao, *Sci. Rep.*, 2015, **5**, 17727.
90 A. M. Aslandaş, N. Balcı, M. Arık, H. Şakiroğlu, Y. Onganer and K. Meral, *Appl. Surf. Sci.*, 2015, **356**, 747–752.
91 R. Bandi, B. Reddy Gangapuram, R. Dadigala, R. Eslavath, S. S. Singh and V. Guttena, *RSC Adv.*, 2016, **6**, 28633–28639.
92 Y. Xiong, M. Chen, Z. Mao, Y. Deng, J. He, H. Mu, P. Li, W. Zou and Q. Zhao, *Crystals*, 2023, **13**, 812.
93 X. Li, Q. Hu, K. Yang, S. Zhao, S. Zhu, B. Wang, Y. Zhang, J. Yi, X. Song and M. Lan, *Sens. Actuators, B*, 2022, **371**, 132534.
94 K. B. Ayaz Ahmed and S. K. Palathedath, *J. Lumin.*, 2016, **177**, 228–234.
95 S. Liao, X. Zhao, F. Zhu, M. Chen, Z. Wu, X. Song, H. Yang and X. Chen, *Talanta*, 2018, **180**, 300–308.
96 M. Zhang, R. Su, J. Zhong, L. Fei, W. Cai, Q. Guan, W. Li, N. Li, Y. Chen, L. Cai and Q. Xu, *Nano Res.*, 2019, **12**, 815–821.
97 R. Purbia and S. Paria, *Biosens. Bioelectron.*, 2016, **79**, 467–475.
98 B. Zhao and Z. Tan, *Adv. Sci.*, 2021, **8**, 2001977.
99 W. Xu, F. Zeng, Q. Han and Z. Peng, *Coord. Chem. Rev.*, 2024, **498**, 215469.
100 Y. Chen, M. Zheng, Y. Xiao, H. Dong, H. Zhang, J. Zhuang, H. Hu, B. Lei and Y. Liu, *Adv. Mater.*, 2016, **28**, 312–318.
101 J. Shao, S. Zhu, H. Liu, Y. Song, S. Tao and B. Yang, *Adv. Sci.*, 2017, **4**, 1700395.
102 H. Jia, Z. Wang, T. Yuan, F. Yuan, X. Li, Y. Li, Z. Tan, L. Fan and S. Yang, *Adv. Sci.*, 2019, **6**, 1900397.
103 J. Guo, H. Li, L. Ling, G. Li, R. Cheng, X. Lu, A.-Q. Xie, Q. Li, C.-F. Wang and S. Chen, *ACS Sustainable Chem. Eng.*, 2020, **8**, 1566–1572.
104 S. Ren, B. Liu, M. Wang, G. Han, H. Zhao and Y. Zhang, *J. Mater. Chem. C*, 2022, **10**, 11338–11346.
105 Y. Pan, L. Qiao, Z. Zhu, X. Ran, Y. Kuang, Z. Chi, Y. He, R. Liu and L. Guo, *Carbon*, 2023, **213**, 118212.
106 Y. Zhang, Y. Liu, X. Ren, Y. Kang, S. Ding and S. Lu, *Angew. Chem., Int. Ed.*, 2025, **64**, e202421421.
107 Y. Zhang, X. Ren, X. Zhao, S. Ding, X. Wu, Y. Liu, X. Zeng, X. Qu, H. Song, Y. Hu, L. Shi and S. Lu, *Adv. Mater.*, 2025, **37**, 2420197.